Use Of Pt/Mesoporous Silica from Silica Beach Sand for Hydrocracking of Castor Oil and Reusability

Siti Salamah[1], Wega Trisunaryanti[2(✉)], Indriana Kartini[2], and Suryo Purwono[3]

[1] Department of Chemical Engineering, Faculty of Engineering, Universitas Ahmad Dahlan, Yogyakarta, Indonesia

[2] Department of Chemistry, Faculty of Mathematics and Natural Sciences, Universitas Gadjah Mada, Yogyakarta, Indonesia
wegats@ugm.ac.id

[3] Department of Chemical Engineering, Faculty of Engineering, Universitas Gadjah Mada, Yogyakarta, Indonesia

Abstract. Biofuel is essential in addressing petroleum-based fuel issues. The most widely used biofuels are vegetable oils. One of the processes to convert vegetable oil into fuel is hydrocracking which requires a catalyst with good activity. This research studied platinum-based mesoporous silica (MS) catalyst in hydrocracking castor oil. The catalysts Pt/MS were synthesized by wet impregnating mesoporous silica from beach sand and standard silica (SBA-15) with platinum (Pt) metal of 15wt%, and were denoted as Pt/MS and Pt/SBA-15 catalysts. The characterization, activity, and reusability of these catalysts in hydrocracking castor oil were evaluated. The hydrocracking process was done in hydrocracking reactor at 450 °C for 2 h and was run for 4 times for its reusability. The results showed that MS and Pt/MS catalysts have specific surface areas of 122 m^2/g, 273.9 m^2/g, respectively, compared to standard Pt/SBA-15 of 436 m2/g. The average pores were 4.65 nm, 3.9 nm, and 7.63 nm. The catalysts showed a crystal diffractogram pattern with crystal peaks appearing at $2\theta = 39$; 46°, 67° and 80°. The liquid fractions produced from the hydrocracking process of MS, Pt/MS, and Pt/SBA-15 were 41.2–46 wt.%, 48.4–50.9 wt.%, and 45.3–47 wt.% with total yield of 84.8–93.8 wt.%, 79–90 wt.%, and 79–89.8 wt.%, respectively, and with a reusability until 4 times. These results showed that Pt/MS catalyst has great performance with reusability until 4 times and still produce product of 79–93.8 wt.%.

Keywords: Platinum · Catalyst · Mesoporous silica · Castor oil · Reusability

1 Introduction

The search for a possible alternative to energy sources has been profoundly explored concurrently with the arising concern of fossil fuels. [1]. One way to overcome the increasing demand for energy from fossil fuels is to look for alternatives to petroleum substitutes, such as biofuel [2]. Biofuels as an alternative energy source have many

G. W. Bhawika et al. (Eds.): IConBEM 2022, AEBMR 249, pp. 180–191, 2023.
https://doi.org/10.2991/978-94-6463-216-3_14

advantages related to environmental concerns and increased energy security [3]. Plant derived oil, especially nonedible oil, such as castor oil, contain triglyceride that can be converted into biofuel [2–4]. Castor oil exhibits excellent flash point, pour point, and kinematic viscosity [5].

The main component of castor oil is ricinolein acid, with little of oleic acid and palmitic [6]. Processing of castor oil into quality fuel oil can be done through the hydrocracking process [7]. Hydrocracking consists of two combined processes between a cracking process that has a dual function: a metal component as a hydrogenation catalyst and an acid component as a cracking catalyst. Widely used catalyst in the hydrocracking process are metal loaded catalysts [8]. The choice of this load catalyst must consider the properties of the carrier material itself, such as high thermal stability, has a cavity that allows adsorption and has the ability to bind metals as a catalyst. Among the many existing catalysts, mesoporous silica has attracted much attention in recent years due to its high porous nature and better performance [9]. A mesoporous material is defined as a material with a pore size between 2–50 nm. The mesoporous structure can solve and avoid the diffusion limitation of large molecules during catalysis; therefore, better catalyst activity can be expected [10].

Mesoporous materials [MS] can be synthesis used a metal oxide in surfactant, the next step by the remove of surfactant [9]. The silica from Parangtritis beach sand was extracted and utilized to synthesize mesoporous silica. The synthesis of MS utilized dodecyl amine (DDA) as a template by solgel method [11].

Metal precursors are required to increase the number of active sites in a catalyst, thus increasing the activity and selectivity of the catalyst. This study impregnated platina (Pt) as metal precursors to support MS catalyst. By impregnating platinum, it is expected to increase the number of active sites and ability of the catalyst, thereby increasing the catalytic performance. Platinum is transition metals, if it is loaded on the material that becomes a catalyst, it supports for high selectivity [7].

This paper studied the synthesis of mesoporous silica from beach sand as a platinum supported catalyst. The synthesis was done using a dodecyl-amine (DDA) template through sol-gel method, The platinum was then impregnated using wet impregnation method with variations of platinum content weight of 5 wt.%. The catalysts were assessed for the activity in the hydrocracking process of Castor oil to biofuel.

The results were compared to the catalyst from standard synthetic mesoporous silica (SBA-15) [12].

2 Methods

2.1 Materials

The sand was collected from beach sand. Distilled water, hydrochloric acid (HCl 37%, Mallinckrodt), NaOH from PA VWR Chemicals, $AgNO_3$, pyridine from Sigma Aldrich. $C_{12}H_{27}N$ from Fisher Scientific. $PtCl_2$ from Sigma Aldrich.

2.2 Methods for Sample Preparation

The synthesis of MS from beach sand containing SiO_2 utilized DDA surfactant as the template. To obtain soluble sodium silicate, SiO_2 was dissolved in 1.5 M NaOH solution.

At 40 °C for 30 min, 0.5 g of DDA was dissolved in 25 ml solution of 1:1:1 mixture of solvent, distilled water, and ethanol. At 29 °C, sodium silicate was added dropwise to the DDA solution at a rotation speed of 120 rpm. Allow the mixture to stand for 1 h and add 6 M H_2SO_4 to achieve a pH of 5. The mixture was kept at room temperature for 18 h. The product was filtered and rinsed with distilled water until the pH reached 6, then dried for 4 h at 50 °C. To remove the template, the dry products were calcined at 600 °C for 5 h at a heating rate of 5 °C/min [11].

2.3 Preparation Catalyst

The catalyst Pt/MS from mesoporous silica (MS) was prepared by impregnating platinum chloride in a ratio of 5 wt. % to MS for 24 h at a temperature of 30 °C, then drying for 24 h at 100 °C. Next, the catalyst calcined at a temperature of 500 °C for 5 h with nitrogen gas and reduced for 4 h at 450 °C with a hydrogen gas stream [11].

2.4 Characterization

The existence and absence of functional groups in Pt/MS were analyzed utilizing Fourier Transform Infrared Spectrometer (FTIR). The sample was used to analyze the acidity with Gravimetric method. The acidity was determined according to the following formula,

$$\text{Acidity} = \frac{\text{WA}}{\text{W}_\text{B} \times \text{M}_{C5H5N}} \times 1000 \frac{\text{mmol}}{\text{g}}$$

Here, W_A is the weight of adsorbed pyridine vapor (g), W_B is the mesoporous silica weight, and M_{C5H5N} is the Mr of pyridine (79.01 g/mol).

The catalys character were analyzed using a N_2 gas sorption analysis performed with a Quantachrome NOVA touch. The total surface area was calculated using the BET method. The pore size distribution was estimated using the BJH desorption model. The crystallinity of the mesoporous silica was analyzed using X-ray diffraction (XRD) on a Rigaku Miniflex 600 with a monochromatic Cu Kα radiation source (λ = 1, 5 °A), 30 kV, 10 mA, scan speed 10° min^{-1} and scan range of 2–80°. The morphology of catalyst was characterized using Scanning Electron Microscope (SEM) and Transmission Electron Microscope (TEM).

The hydrocracking of castor oil was performed by adding 0.2 g of Pt/MS to the catalyst vessel and 10 g of castor oil to the oil vessel. Samples and catalyst were put into the hydrocracking reactor. The reactor was adjusted to a temperature of 450 °C for 2 h with a hydrogen gas flow rate of 20 ml/min. The catalytic activity of mesoporous silica was evaluated during the hydrocracking of castor oil. The liquid produced during hydrocracking was analyzed by gas chromatography-mass spectrometer (GCMS) [9].

The yield product was determined by used calculation as written in the equation below [13]:

$$Yield\,(wt.\%) = \frac{Wp}{WF} x100\% \quad (1)$$

$$Residue(wt.\%) = \frac{WR}{WF} x100\% \tag{2}$$

$$Coke(wt.\%) = \frac{WC2 - WC1}{WF} x100\% \tag{3}$$

$$Gas = 100\% - (yield + Residue + Coke) \tag{4}$$

$$Totalyield = (100\% - Residue) \tag{5}$$

$$Selectivity(wt.\%) = \frac{Ac}{At} x100\% \tag{6}$$

Here, Wp is the product weight, WF is the feed weight, WR is the unconverted product weight (g), WC is the weight of catalyst before (WC_1) and after (WC_2) hydrocracking (g), Ac is GC-MS area of the compound, and At is the total GC-MS area.

3 Results and Discussion

3.1 Characterization of Pt/MS Catalyst

The catalysts used were defined MS for mesoporous silica, Pt/MS and Pt/SBA-15 for the standard Pt/MS. The samples characterized by FTIR, as shown in Fig. 1. The broadband at a wave number of 460–3447 cm^{-1} was shown. The bending vibration was detected at a wavenumber of 470 cm^{-1}, indicating the presence of Si-O-Si. An influentially strong intensity band of 1095 cm^{-1} represented H-O-H bending, this was due to the interaction of the O-H group derived from water on the surface of the Pt/MS via hydrogen bonds. It was well known that 450 – 1300 cm^{-1} range was the unique silica band [9]. The broadband at a wavenumber of 1635 cm^{-1} showed Si-OH bending as there was a new band at 1635 cm^{-1} and a strong band at 3448 cm^{-1}.

This phenomenon is in accordance with the study [13]. The broadband at a wavenumber of spectra MS and Pt/SBA-15, which represented water O-H bending and O-H stretching, represented silanol (Si-OH) and Siloxane functional (Si-O-Si), respectively [6]. The impregnation process of Pt does not destroy or affect the functional group of MS. In addition, the FTIR result does not show any Ni peak, because metal elements will only appear in fingerprint area.

3.2 Acidity Test

The acidity test with gravimetric method was used to determine the acidity of the MS surface. Pyridine was an alkaline absorbed by a mesoporous material with acid sites in its framework. The acidity result for MS, Pt/MS, and Pt/SBA-15 were 0.68 mmol/g, 1.4 mmol/g, 2.03 mmol/g, respectively. The Bronsted and Lewis acid sites function as proton donors and electron pair acceptors, respectively [6]. The higher the acidity of the Pt/MS catalyst indicated its potential as a catalyst in processes requiring acid sites, such as hydrocracking. The more platinum loaded into the MS increases the acidity. This is due to uneven pore distribution on the surface of the material [6].

Table 1. The Characteristic of the catalyst

Samples	Specific Surface Area (m^2/g)	Total pore volume (cc/g)	Average Pore Diameter (nm)
MS	122.8	0.14	4.65
Pt/MS	237.9	0.23	3.9
Pt/SBA-15	436.6	0.83	7.63

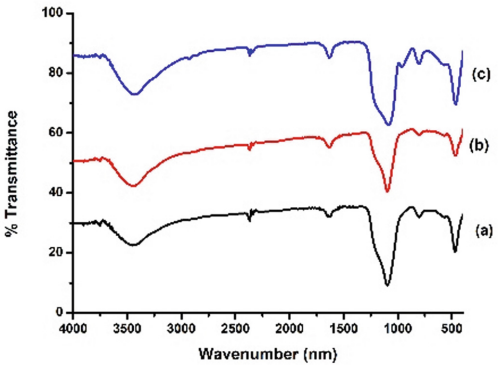

Fig. 1. Infra-Red of (a) MS (b) Pt/MS and (c) Pt/SBA-15

3.3 Gas Sorption Analysis

The porosity of Pt/MS and Pt/SBA-15 catalyst were determined using Gas Sorption Analyzer (GSA). The BET equation was used to calculate the isotherm graph and specific surface area. The BJH model was used to calculate pore volume, mean pore diameter, and pore size distribution. The results of GSA characterization determine the classification of mesoporous materials according to their pore size [9]. Table 1 shows the results of the GSA characterization.

All samples were mesoporous, 2–50 nm with the synthesized Pt/MS catalysts has 3.9 nm pore diameter. Despite the fact that platinum-free MS was in the mesoporous range, its pore volume was shallow in comparison to Pt/MS and Pt/SBA-15, suggesting low porosity formation. It was discovered that the platinum loading influences the formation of porosity during catalyst synthesis. The greater the number of templates used, the greater the porosity properties, i.e., specific surface area and pore volume. This phenomenon is consistent with the findings by Cho et al. [15].

The Pt impregnation into MS increases the surface area of MS; the larger the Pt is carried, the wider the surface area has become. For example, for 5 wt. % Pt, there is an increase of 90% in the surface area. While Pt/SBA-15 has a surface area of 436.6 m^2/g. As the surface area increases, more reactants are adsorbed, and the possibility of a reaction occurring is greater. The impregnation of Pt causes the increase in the physical properties of the catalyst into the MS pores as the entry of Pt into the carrier increases the active site.

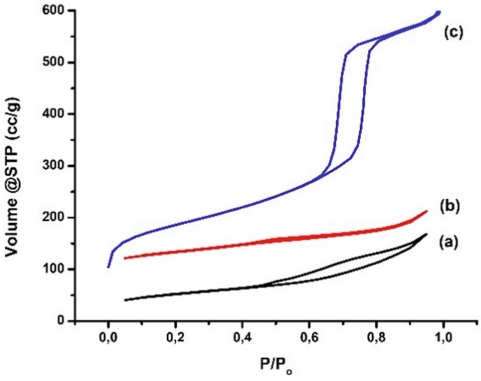

Fig. 2. Nitrogen sorption isotherm of (a) MS (b) Pt/MS and Pt/SBA

Isotherm graphic for both Pt/MSA and MSB was depicted in Fig. 2. The presence of the hysteresis loop confirmed the presence of mesoporous structure in both MS and Pt/MS. These isotherm patterns were similar to the IUPAC type IV isotherm model, except for the hysteresis loop which was similar to type H4. The hysteresis loop of type H4 was well known for materials with narrow slit-like pores, particles with irregular internal voids, and wide distribution size [9].

3.4 Catalyst Crystallinity

The Catalyst crystallinity was examined used XRD visualized in Fig. 3. From the XRD, **i**t was found that MS has an amorphous silica mesoporous phase [11]. While catalyst with impregnated Pt 5%, showed crystals. This was because the increase in the metal content of Pt produced a crystal diffractogram pattern with crystal peaks appearing at $2\Theta = 40; 47^{\circ}$, and 68 (111), (200),(220) and 311 (JCPDS card no. 01–087-0642). These results indicate that these peaks are characteristic of platinum where the presence of the

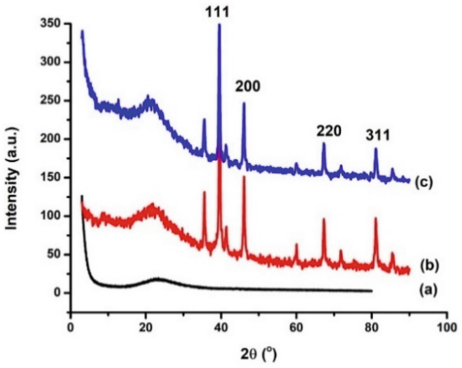

Fig. 3. Diffraction pattern of (a) MS, (b) Pt/MS1 and (c) Pt/SBA-15 catalyst.

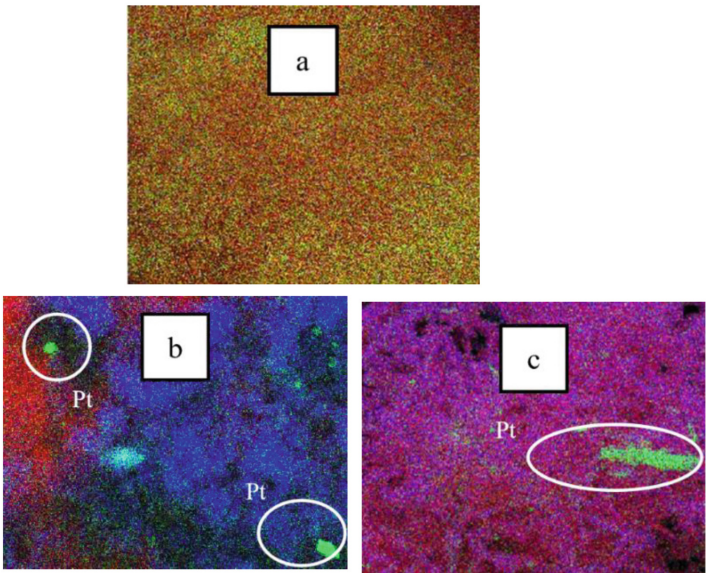

Fig. 4. EDX-Mapping morphology of a. MS, b. Pt/MS, and c. Pt/SBA catalyst.

support surface and sufficient Pt forms face centered cubic Pt crystals, which aligns with a research study by Choi. et al.[15].

3.5 Characterization Pt/MS Catalyst with SEM

SEM-EDX Mapping was used to know the morphology of the catalyst structure. SEM-EDX imaging was required to characterize the 3D surface morphology of the catalyst and platinum distribution in MS. Figure 4 depicts catalyst silicas which appear to be linked by intercrystallite joints.

The EDX mapping is a very useful method for examining the distribution of each type of atom on the surface of the catalyst. The EDX spectra, as shown in Fig. 4. Confirms that the main elements of the analyzed material are Silica (Si), Oxygen (O), and platinum (Pt). According to the EDX data, the Pt/MS catalyst material contains a number of elements.

The red, blue, and green dots in the Pt/MS catalyst are identified as silica, oxygen, and platinum. This demonstrates the evenly distributed Pt atoms. Pt atoms, on the other hand, agglomerates into clusters. The agglomeration is not anticipated because it reduces the surface area of the catalyst, which is expected to interact with the feed during the catalyst activity test. Pt atom precursors are detected both inside and outside of the mesoporous channels.

3.6 Catalytic Activity

The catalyst was assessed as a catalyst in hydrocracking castor oil. Hydrocracking utilizing MS catalyst yields a lower liquid fraction and greater amount of gas product,

whereas Pt/MS catalyst yield the optimal liquid product. This suggests that the amount of Pt loaded in MS affects the property and activity of the catalyst. The liquid fraction yield by the activity of Pt/MS catalyst and Pt/SB-15 catalyst were 47.6 wt.% and 47 wt.%, respectively. This phenomenon could be caused by the acid site location, where the acid site of Pt/MS could reside deep beneath the catalyst. While the feed and product could easily enter and exit the catalyst, the chance of the feed locating the active site before exiting became slimmer. This hypothesis appears to be responsible for the relatively high amount of oxygenated product [9]. The GC-MS analysis of castor oil revealed that it contains 90% stearic acid [15] and carbocyclic acid functional group, necessitating the use of a catalyst with high activity for cracking bonding in structure functional group (Table 3).

The analysis of the chromatogram data produced by the gas chromatography shows the number of components which were separated from the liquid fraction and was detected using a mass spectrometer (MS). The liquid product was obtained from the hydrocracking process of castor oil it was seen Table 2. The analysis from the results of the GC-MS the liquid product contains gasoline and oxygenated product (alcohol, aldehyde, ketone, and carboxylic acid). The liquid produce has selectivity of the gasoline fraction is very low. This is probably because castor oil contains a lot of stearic acid higher. Hydrocracking process through deoxygenation reaction decarboxylation, and decarboxylation reactions [2, 14, 15]. This shows several reactions occur simultaneously in the cracking process with a catalyst that Pt carrier in MS can undergo

Table 2. Hydrocracking products of Castor oil

Hydrocracking catalyst	**Yield (wt.%)**				**Total Yield. (wt.%)**
	Liquid product	**Gas product**	**Residue**	**Coke**	
MS	41.2	51.2	6.2	1.4	93.8
Pt/MS	47.6	21	30.8	0.6	79.5
Pt/SBA-15	47	41.2	10.2	1.6	89.8

Table 3. Product Selectivity of the MS, Pt/M, and Pt/SBA-15 Catalytic hydrocracking of Castor oil

Hydrocracking catalyst	**Liquid fraction (wt. %)**		
	Gasoline (C_5-C_{12})	**Diesel (C_{13}-C_{17})**	**Oxygenated Product**
MS	1.36	0.0	39.84
Pt/MS	1.69	0.0	45.91
Pt/SBA-15	3.7	00	43.94

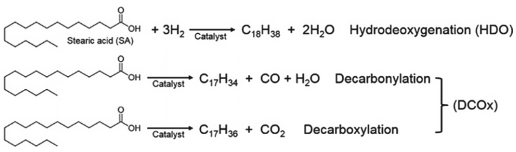

Fig. 5. The step reaction of catalytic deoxygenation [14]

deoxygenation, decarboxylation, and hydrodeoxygenation reactions as shown from the Step reaction in Fig. 5 [14].

The Pt/MS catalyst is the optimal with 40.76% of liquid fraction yield. The cracking is caused by the breaking of the C-C bond and -CHO-. Furthermore, CO_2 by-products are formed through decarboxylation. Following the fatty acid deoxygenation process, the decarboxylation and hydrodeoxygenation reactions often occur through a catalyst. The decarboxylation and decarbonylation reactions occur concurrently to produce alkane and alkene products. It is clear the liquid product is less. According to Choi et al. [14], the degree of deoxygenation in Pt/TiO in hydrocracking castor oil was 36%. This is also likely what happened to the Pt/MS catalyst, resulting in a less gasoline selective active site.

3.7 The Reusability of MS, Pt/MS5, Pt/SBA-15 Catalyst for Hydrocracking of Castor Oil

The reusability of catalyst was investigated in 4 runs of the hydrocracking process of the castor oil at 450 °C for 2 H, as shown in Table 4. During the 4 runs, the catalyst produced a constant result in the conversion. The formation of coke appears to occur at a relatively low rate, suggesting a stability toward coke poising [16]. This particular reusability of Pt/MS and Pt/SBA-15 may be attributed to the presence PtO within the metal structure. The rate of coke formation increases from the 1st to the 4th run. As a result, the catalyst was deactivated.

The liquid product of the Pt/MS catalyst is relatively reduced from 1st to 4th run. This probably due to the uneven distribution of the catalyst metals on the surface caused by high temperatures at which the agglomerated metals melt. Eventually, the distribution of metals becomes more homogeneous as there are more active catalyst sites and the hydrocracking process repeats.

Table 4. Reusability Pt/MS catalyst in Hydrocracking of Castor oil

Catalyst	Product	Running 1	Running2	Running3	Running 4
MS	Residue	6.2	6	7	10
	Liquid	41.2	41	40	39.3
	Coke	1.4	1.7	1.8	2.2
	Gas	51.2	51.6	51.2	48.5
	Conversion	93.8	94	93	90
Pt /MS	Residue	10.4	10	11	21
	Liquid	50.9	51.3	45.8	48.4
	Coke	0.8	1.2	1.8	1.1
	Gas	37.9	37.5	41.4	29.5
	Conversion	89.6	90	89	79
Pt/SBA-15	Residue	10.2	20.2	20.2	21
	Liquid	47	47	45.4	45.3
	Coke	1.6	1.4	1.4	1.8
	Gas	41.2	31.4	33	31.9
	Conversion	89.8	79.8	79.8	79

4 Conclusion

Characteristics and activity analysis of MS and Pt/MS catalyst synthesized from beach sand were conducted. The results showed that MS, Pt/MS, and Pt/SBA-15 catalysts have specific surface areas of 122 m^2/g, 273.9 m^2/g, and 436 m^2/g, respectively while average pores were 4.65 nm, 3.9 nm, and 7.63 nm. The specific surface areas and average pores of MS and Pt/MS were lower compared to Pt/SBA-15. The catalysts displayed a crystal diffractogram pattern with crystal peaks of the Pt/MS catalyst and Pt/SBA catalyst. The catalysts were tested for their activity as the catalyst in hydrocracking castor oil. The liquid fraction yielded were 47.6 wt.% for Pt/MS catalyst and 47 wt.% for Pt/SBA-15. The liquid fraction is made up of 1.09% gasoline fraction and 45% oxygen product. Despite this, the catalysts were tested for its reusability up to 4 runs with a total yield of 79.5 – 93.8 wt.%.

Acknowledgments. This work was support by The Doctoral Dissertation Research (PDD) grant scheme under contract number 208/UN.1/DITLIT/DITLIT/PT/2021.

Authors' Contributions. First Author: data collection and analysis, writing the draft manuscript.
Correspondent Author: proofreading the manuscript.
Co-Author: Investigation research and data analysis consultant.

References

1. W. Trisunaryanti, K. Wijaya. Triyono. A. Rahma A., S. Larasati, "Green Synthesis of Hierarchical porous Carbon prepare from coconut lumber sawdust as Ni based catalyst support for hydrocracking *Callophyllum inophyllum* oil", Resulting Engineering,11,100258, pp.1–12,202. https://doi.org/10.1016/j.rineng.2021.100258
2. M. Molefe, D. Nkazi, and H. E. Mukaya, "Method Selection for Bio jet and Bio gasoline Fuel Production from Castor Oil: A Review," *Energy and Fuels*, vol. 33, no. 7, pp. 5918–5932, 2019, https://doi.org/10.1021/acs.energyfuels.9b00384.
3. D. Verma, B. S. Rana, R. Kumar, M. G. Sibi, and A. K. Sinha, "Diesel and aviation kerosene with desired aromatics from hydro processing of jatropha oil over hydrogenation catalysts supported on hierarchical mesoporous SAPO-11," *Appl. Catal. A Gen.*, vol. 490, no. 1, pp. 108–116, 2015, https://doi.org/10.1016/j.apcata.2014.11.007.
4. S. Liu, Q. Zhu, Q. Guan, L. He, and W. Li, "Bio-aviation fuel production from hydro processing castor oil promoted by the nickel-based bifunctional catalysts," *Bioresour. Technol.*, vol. 183, pp. 93–100, 2015, https://doi.org/10.1016/j.biortech.2015.02.056.
5. R. Yang *et al.*, "Transformation of Jatropha Oil into High-Quality Biofuel over Ni-W Bimetallic Catalysts," *ACS Omega*, vol. 4, no. 6, pp. 10580–10592, 2019, https://doi.org/10.1021/acsomega.9b00375.
6. K. Wijaya, A. D. Ariyanti, I. Tahir, A. Syoufian, A. Rachmat, and Hasanudin, "Synthesis of Cr/Al_2O_3- Bentonite Nanocomposite as the Hydrocracking Catalyst of Castor Oil," *Nano Hybrids Compos.*, vol. 19, pp. 46–54, 2018, https://doi.org/10.4028/www.scientific.net/nhc.19.46.
7. T. Hanaoka, T. Miyazawa, K. Shimura, and S. Hirata, "Jet fuel synthesis in hydrocracking of Fischer-Tropsch product over Pt-Loaded zeolite catalysts prepared using microemulsions," *Fuel Process. Technol.*, vol. 129, pp. 139–146, 2015, https://doi.org/10.1016/j.fuproc.2014.09.011.
8. E. Meller, V. Gutkin, Z. Aizenshtat, and Y. Sasson, "Catalytic Hydrocracking -Hydrogenation of Castor Oil Fatty Acid Methyl Esters over Nickel Substituted Polyoxometalate Catalyst," *ChemistrySelect*, vol. 1, no. 20, pp. 6396–6405, 2016, https://doi.org/10.1002/slct.201601030.
9. Salamah S., Trisunaryanti W., Kartin I., Suryo Purwono,2021, Hydrocracking Of Waste Coconut Oil Into Biofuel Using Mesoporous Silica From Parangtritis Beach Sand Synthesis By Sonochemistry, *Silicon Journal*, https://doi.org/10.1007/s12633-021-01117-0
10. J. Zhao, G. Wang, L. Qin, H. Li, Y. Chen, and B. Liu, "Synthesis and catalytic cracking performance of mesoporous zeolite y," *Catal. Commun.*, vol. 73, pp. 98–102, (2016), https://doi.org/10.1016/j.catcom.2015.10.020
11. Salamah,S.,Trisunaryanti,W., Kartini, Purwono, S. (2021), "Synthesis and characterization of mesoporous silica from beach sand as silica source", Proseding The 4 th International conference On Chemical & Material Engineering, IOP.Conf.Series: Material Science and Engineering Indonesia. https://doi.org/10.1088/1757-899X/1053/1/012027.
12. K. Jaroszewska, A. Masalska, D. Czycz, and J. Grzechowiak, "Activity of shaped Pt/AlSBA-15 catalysts in n-hexadecane hydroisomerization," *Fuel Process. Technol.*, vol. 167, pp. 1–10, 2017, https://doi.org/10.1016/j.fuproc.2017.06.012.
13. Trisunaryanti W.,Sumbogo,S.,D., Mukti.,R.,R.,Kartika.,I.A.,Hartati.,Triyono.2021, Performance of low-content Pd and high-content Co, Ni supported on hierarchical activated carbon-for the hydrotreatment of Calophyllum inophyllum oil (CIO).Reaction Kinetic,Mechanisme and catalysis. https://doi.org/10.1007/s11144-021-02060-2
14. F. Zaher, A. E. S. Hussein, H. Hassan, and S. F. Hamed, "Potential of Castor Oil as a Feedstock for the Production of Bio-fuel via Catalytic Hydro- Cracking," *Curr. Sci. Int.*, vol. 4, no. July, pp. 443–449, 2015.

15. I. H. Choi, J. S. Lee, C. U. Kim, T. W. Kim, K. Y. Lee, and K. R. Hwang, "Production of bio-jet fuel range alkanes from catalytic deoxygenation of Castor fatty acids on a WOx/Pt/TiO2 catalyst," *Fuel*, vol. 215, no. June 2017, pp. 675–685, 2018, https://doi.org/10.1016/j.fuel.2017.11.094.
16. Alisha G. ,D., Trisunaryanti, W., Soufian, Larasati (20021), Biomasa Convertion and Biorefinary, https://doi.org/10.1007/s13399-021-02064-x